A very short introduction to the Kangerlussuaq watershed

Keld Rømer Rasmussen

Summer 2018

Background

Several studies have dealt with the hydrology of the area between Kangerlussuaq and the Greenland Ice Shield (GrIS). Based on some of these I have extracted information for the participants of the Aarhus Geoscience 2018 "Greenland Excursion to the Kangerlussuaq area". The aim of this short note is to give insight in hydrology of the Watson river catchment upstream the road bridge in Kangerlussuaq (Figure 1). This will include some quantitative information of the elements of the water balance and mass balance of the catchment. A secondary aim is to provide basic insight in some of the challenges of performing reliable hydrometry observations in glacial rivers. Because of copyright issues this note is for internal use only.

Figure 1. View of the bridge across the Watson River in Kangerlussuaq as seen from the summit of "Ravneklippen" (Raven-peak) south of the river. Note that the stream passes the bridge in a northern (deep) and two southern (shallower) channels. The northern and middle channels have both been partly excavated using explosives. The mid and southern sections of the bridge were built after a catastrophic flood partly destroyed the existing bridge in 2012 (One of several videos of the collapse is available at https://www.youtube.com/watch?v=kKjXKAatiIs) .

The Watson River Catchment

Delineating a catchment which partially drains areas from an ice cap is uncertain. The discharge station at Kangerlussuaq (Søndre Strømfjord) receives streamflow from 2 major valleys: Sandflugtsdalen and Ørkendalen (Fig. 2a).

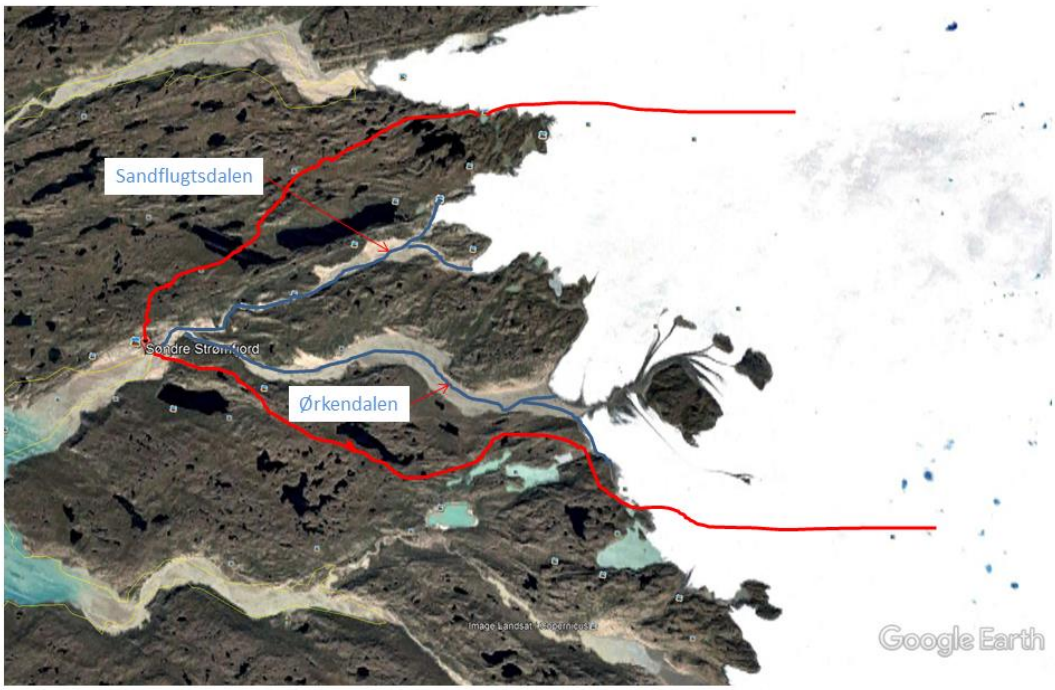

Figure 2a. The Watson River catchment (Kangerlussuaq) with tributaries from the two major valleys Ørkendalen and Sandflugtsdalen.

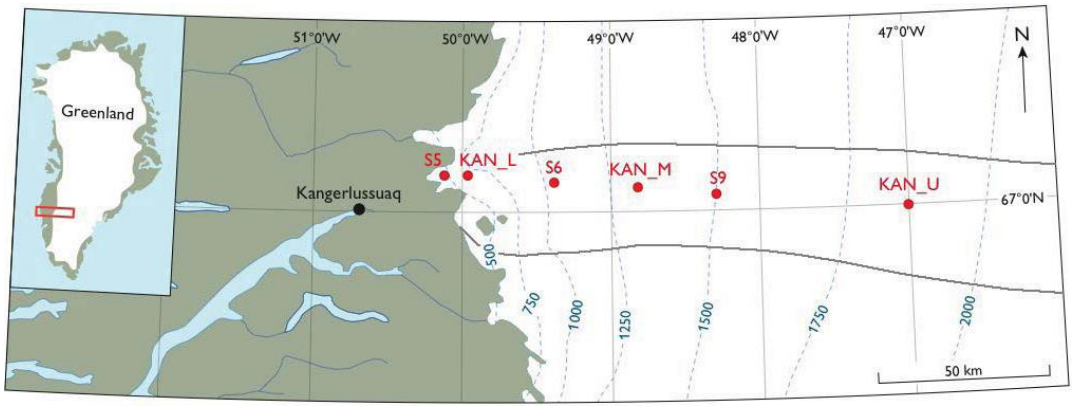

Figure 2b. The extension of the catchment on the Greenland Ice Shield (GrIS) east of Kangerlussuaq. The two grey lines delineate the catchment to the North and the South. Red dots indicate climate stations on GrIS.

In the upstream parts of the two valleys meltwater streams receive runoff from outlet tongues coming from the Ice Cap. The area of the ice-free part of the catchment is approximately 550 km^2, while when including the ice covered part as indicated in Figure 2b the area is about 12000 km^2 (Lindbäck et al., 2015). While this area is relevant when studying the annual balance the area contributing to streamflow at any particular season varies as the supra (on the ice) as well as the englacial (within the ice) drainage systems grow or shrink. Further water subglacially contributes to the discharge.

Temperature, precipitation and evaporation

For the period 1973-1999 the average temperature at Kangerlussuaq airport was -5.7°C and the temperature typically varied from -25°C to 16°C and was rarely below -36°C or above 20°C (Cappelen et al., 2000). The daily average was typically above 0 °C from the beginning of May to the end of September (Figure 3). Between 2000 and 2016 the average annual temperature at Kangerlussuaq increased to -3.4°C (Cappelen et al., 2017).

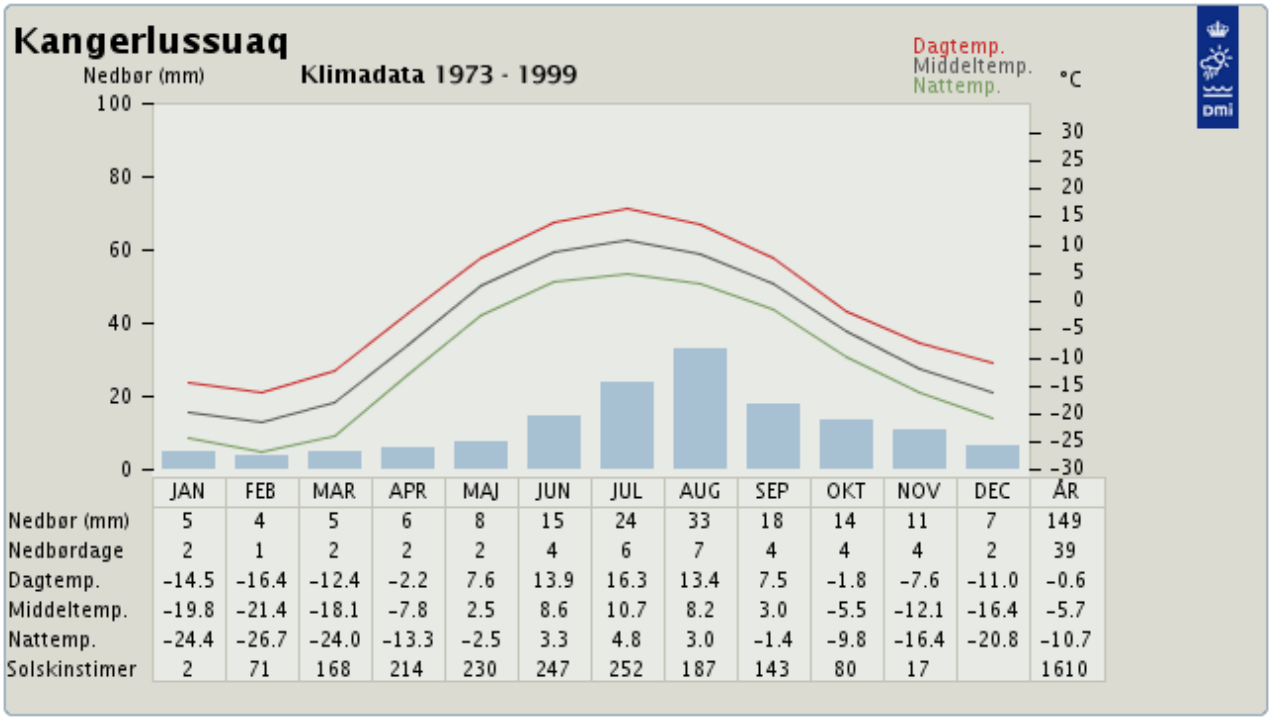

	JAN	FEB	MAR	APR	MAJ	JUN	JUL	AUG	SEP	OKT	NOV	DEC	ÅR
Nedbør (mm)	5	4	5	6	8	15	24	33	18	14	11	7	149
Nedbørdage	2	1	2	2	2	4	6	7	4	4	4	2	39
Dagtemp.	-14.5	-16.4	-12.4	-2.2	7.6	13.9	16.3	13.4	7.5	-1.8	-7.6	-11.0	-0.6
Middeltemp.	-19.8	-21.4	-18.1	-7.8	2.5	8.6	10.7	8.2	3.0	-5.5	-12.1	-16.4	-5.7
Nattemp.	-24.4	-26.7	-24.0	-13.3	-2.5	3.3	4.8	3.0	-1.4	-9.8	-16.4	-20.8	-10.7
Solskinstimer	2	71	168	214	230	247	252	187	143	80	17		1610

Figur 3. Climatological standards, 1973-1999 (http://www.dmi.dk/groenland/arkiver/klimanormaler/). Note that precipitation is uncorrected.

For the period 1981-2012 the annual precipitation expressed as water equivalent was near 250 mm at Kangerlussuaq i.e. at the outlet of the watershed (Mernild et al., 2015). Precipitation during summer and autumn was higher than during winter and spring. In their analysis, a bias correction factor of 1.46 was used for the annual precipitation. Using the same bias correction factor and observations from Kangerlussuaq airport (Cappelen, 2017) the annual precipitation for the period 1973-1999 and 2000-2016 was 218 mm respectively 232 mm, indicating a small (6%) increase during the latest period.

Less data exist for the larger parts of the GrIS-parts of the watershed. Here Mernild et al. (2018) have, assisted by model calculations derived the precipitation-elevation relationship shown in Figure 4.

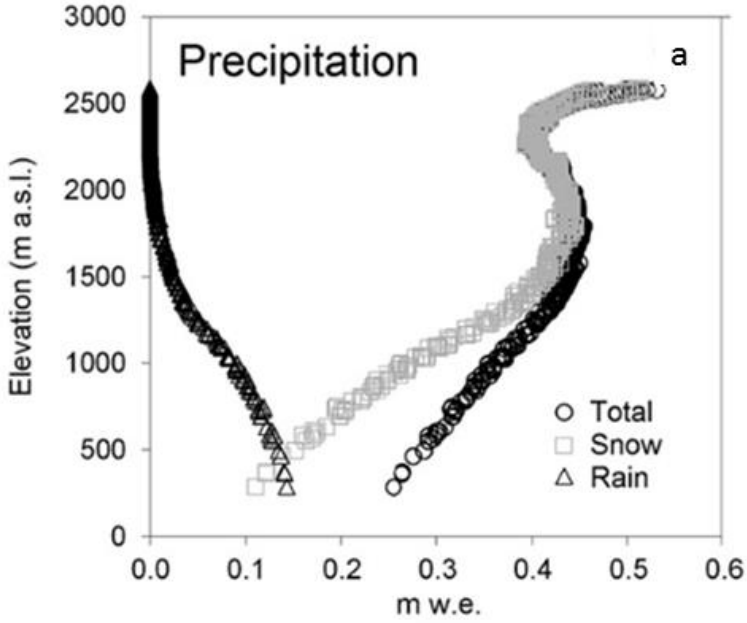

Figure 4. The precipitation-elevation relationship for the Kangerlussuaq part of GrIS;

Using the relationship shown in Figure 4 they have estimated the annual precipitation on the entire watershed as shown in Figure 5. It should be seen that this is about 400 mm (water equivalent).

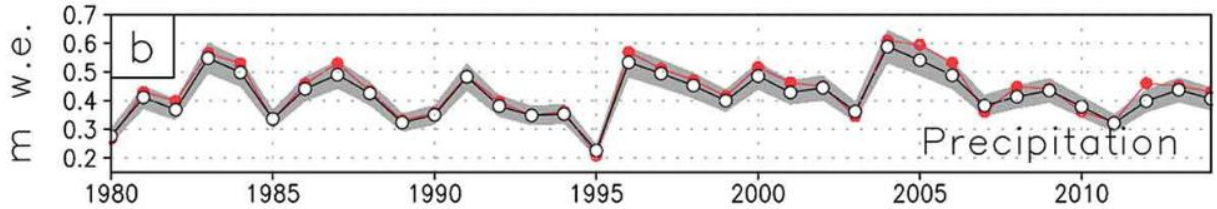

Figure 5. Estimated precipitation from 1980-2014 on the Kangerlussuaq watershed – values are corrected for systematic losses due to evaporation from the gauge and loss due to wind influences (Mernild et al. 2018).

The long-term annual evaporation from the watershed is estimated to about 100 mm. Therefore, the major part of precipitation will leave the watershed as meltwater in the Watson River.

The energy/mass balance

Hydrology in the area links closely to the short and long wave radiative fluxes. This controls, for instance, the strong diurnal and annual variations of discharge. While sensible and latent heat fluxes may play a role outside GrIS, these almost cancel each other on the GrIS - in particular above the equilibrium line (Ambach, 1963).

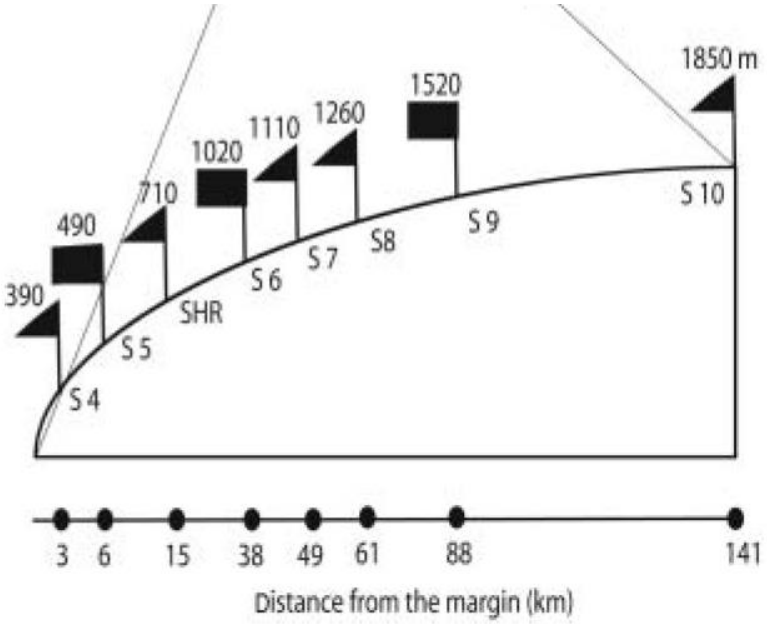

Figure 6. Mass balance stations along the Kangerlussuaq transect. Numbers above the flags indicate elevation. Distance from the ice margin is shown below (van de Wal et al., 2005).

On the ice sheet NE of Kangerlussuaq mass balance measurements have been performed at approximately 1010 m elevation at the profile shown on Figure 6 (The Kangerlussuaq transect). Table 1 presents some important meteorological variables measured on a mast at the station during the period 1998-2002. The table shows that the annual net radiation is 130 W/m^2 – 95 W/m^2 = 35 W/m^2 which is balanced by a similar, but negative difference in net long wave radiation (-36 W/m^2). At Kangerlussuaq at ~25 m elevation the daily net radiation between primo May and mid-August is typically around 200 W/m^2 or almost twice the value of the average annual incoming short wave radiation. Overall, this quantity governs the amount of meltwater generated on the ice cap and thus the loss of ice due to melting.

	1998	1999	2000	2001	2002	1998–2002
Temperature (°C)	–10.1	–10.8*	–11.3	–10.4	–10.7	–10.6
Wind speed (m s^{-1})	6.4	5.9*	6.3#	6.1	5.8	6.1
S_{in} (W m^{-2})	124	135	134	131	128	130
$S_{reflected}$ (W m^{-2})	88	96	96	100	94	95
L_{in} (W m^{-2})	236	230*	232	231	–	232+
L_{out} (W m^{-2})	270	266*	266	269	–	268+
R_{net} (W m^{-2})	0	3	3	–7	–	0+

*No data in November. #No data over the months March–July. +1998–2001.

Table 1. Meteorological annual mean values on the ice cap at 1010 m asl.

van de Wal et al. (2005) measured the annual mass balance at each of the stations shown in Figure 5. When doing so one may for instance consider the annual incoming and outgoing fluxes for a 1 m

wide section having length L where L is the annual horizontal displacement of the ice resulting from the displacement velocity V at this particular location. The rock below the glacier and the ice surface on top of the volume confine its vertical extent (Figure 7). We assume annual values of our variables at a steady state condition. Now consider one year with a given mass contained by the control element marked by symbols L, H_i and H_u (left element on Figure 7). At the same year the adjacent element in the upstream direction is contained by symbols L, H_{i-1} and H_{u-1} (right element on Figure 7). Now, if there were no mass-loss due to melting, then during the following year the control element to the right would be displaced to the position marked by L, $H_{i,-1}$ and $H_{u,-1}$.

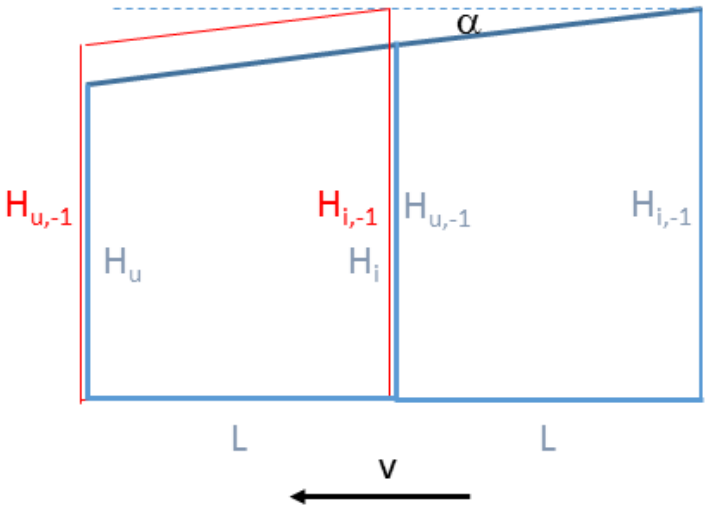

Figure 7. Control element on the ice cap.

Now melting takes place which in the steady state case must correspond to the difference in ice-mass between the "red" and "blue" control elements to the left. When the surface slope (α) of the glacier is small then L × (H_i-H_u) approximates well the corresponding volume of ice melting (VIM). Since H_i-H_u can also be expressed as $|L \times \tan\alpha|$ we get

$$VIM = L \times |L \times \tan\alpha|$$

Assuming that ice density (ρ_{ice}) within the control volume is invariant from year to year then the loss due to melting (M) expressed as an equivalent column of water (m) melting and ice density is ρ_{ice} we get

$$M = \rho_{ice} \times |L \times \tan\alpha|$$

Based on this type of calculations Table 2 shows the mass balance in m water column at the different elevations on the glacier. Near the front of the glacier, the annual loss is about 4 m while the position of the equilibrium line is near 1500 m.

Elevation masl.	340/390	490	710	1020	1110	1260	1520	1850
Mean 1990-2003 (m)	-4.03	-3.46	-2.92	-1.60	-1.29	-0.68	0.03	0.26

Table 2. Surface mass balance along the K-transect at 67° N.

Based on this type of calculations Table 2 shows the mass balance in m water column at the different elevations on the glacier. Near the front of the glacier, the annual loss is about 4 m while the position of the equilibrium line is near 1500 m.

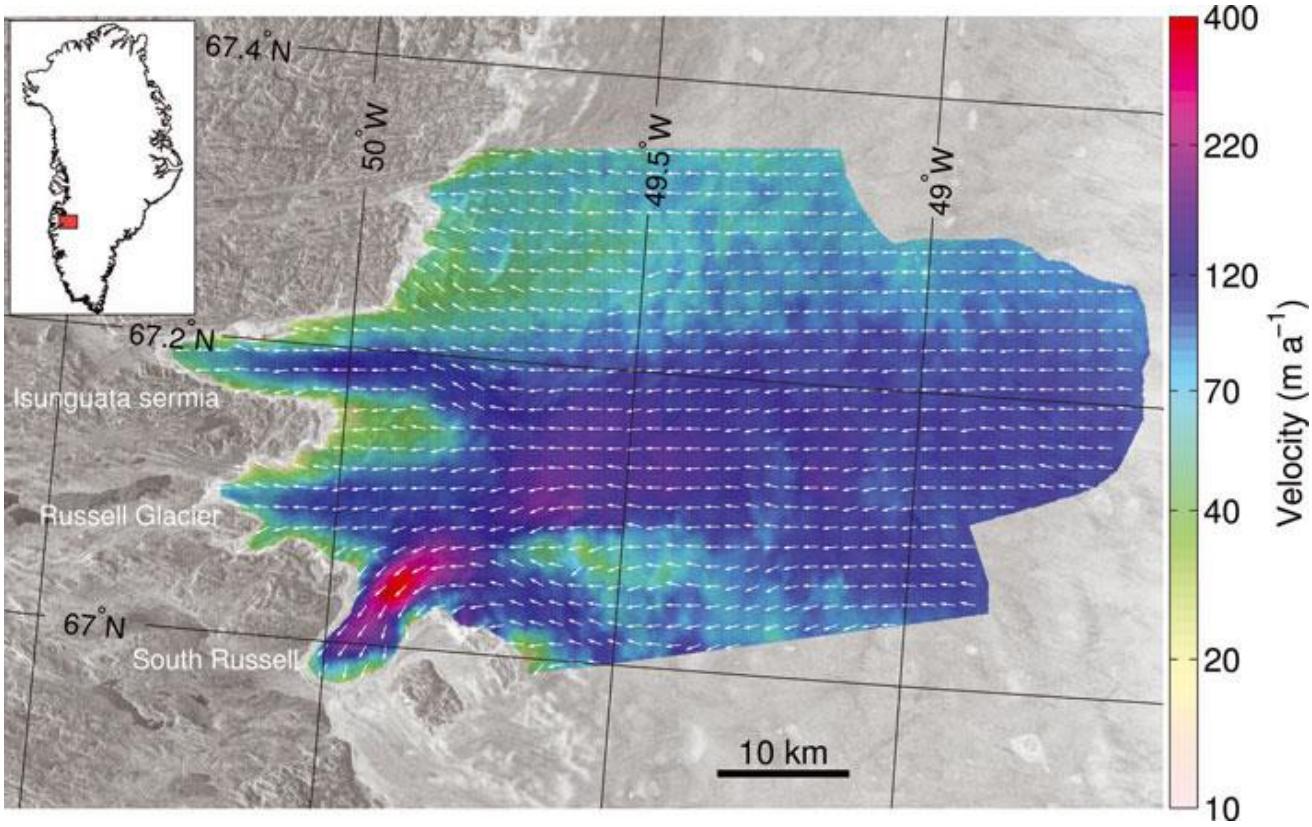

Figure 8. Surface velocity on GrIS east of Kangerlussuaq.

Velocities (direction and speed) of the ice surface are shown on Figure 8. The figure shows that on the central parts of the glacier the surface velocity is mostly of the order of 100 m/year. Lower values are found to the sides and near the protruding bedrock between Russells Gletcher and Isunguata Sermia. Very high values are observed on South Russell.

Figure 9. View of the Watson during late winter 2016. X marks KISS where in summertime water flows right beneath the steep bank and erodes this at maximum discharge.

For the mass loss, the use of annual values masks that the loss takes place during the summer months where the incoming solar radiation peaks. Figure 9 shows a photo of the Watson upstream of Kangerlussuaq during March 2016. During winter the stream channels falls dry apart from some ice on the lowest parts. Therefore, the sediments on the channel bed lies exposed to wind erosion during the entire winter.

For the period 2006-2017 the daily discharge in m^3/s is presented in Figure 10 versus day of year (DOY). Typically, runoff starts between DOY 100 and DOY 150, i.e. during May while it ceases during October approximately between DOY 270 and DOY 290. The figure also shows that discharge peaks between DOY 190 and DOY 220, i.e. near the maximum of incoming solar radiation at summer solstice. Maximum discharge is of the order of 2000 m^3/s, but a few years show higher values. The peak flow for the 12-year period occurred during July 2012 when more than 3100 m3/s swept away the southern section of the bridge on 21. July.

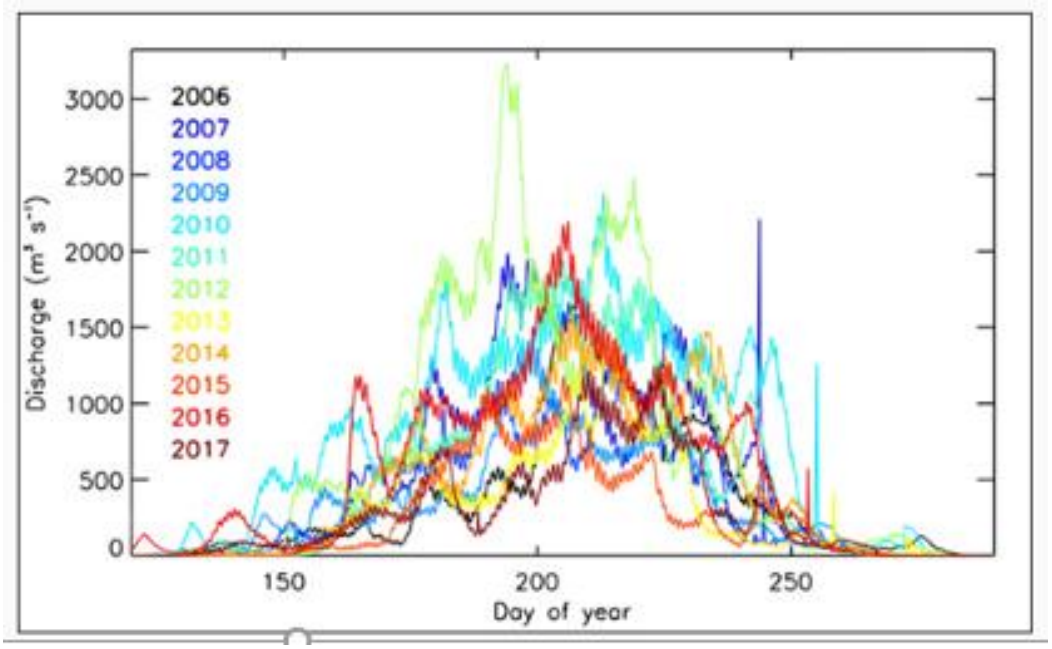

Figure 10. Daily discharge measured at the Bridge in Kangerlussuaq from 2006-2017.

The discharge varies considerably during the summer period. Overall it responds quickly on high solar radiation that results in high ice melting rates. However, the drainage response changes during the summer period as the glacier drainage systems enlarge and become more efficient. Large supra-glacial lakes usually build up on the ice cap during summer time (Figure 11). As these expand and occasionally connect to a particularly widespread and efficient drainage system this may result in extreme discharge events as the 2012-event. Rainfall normally contributes only to runoff at a minor degree. Finally, some short-duration peaks are associated with partial draining of and ice dammed lake in the watershed.

Figure 11. Meltwater lakes on the Greenland Ice Sheet observed from an airplane during summer 2012 (Tyler Jones). Unfortunately, the picture has no scale.

Hydrometry

Continuous recording of the stage in Watson River at the bridge in Kangerlussuaq was initiated in 2006 in order to calculate runoff from the watershed (Mernild & Hasholt, 2009). However, before this can be made one must establish a rating curve, which is the relationship between depth and discharge at the station. The rating curve combines (frequent) manual control measurements of the discharge at the bridge to readings of the stage-board placed (usually) next to the device such as a pressure transducer that records stage. For many rivers, having a regular cross sectional profile, a simple power-expression will fit the data points over the entire depth range. However, the cross section at the bridge in Kangerlussuaq is complex with 3 different channels as pointed out on Figure 1. Furthermore, deepening and widening of the cross sectional geometry of the middle as well as the southern channel took place after the flood that destroyed the bridge in 2012. This resulted in an abrupt change of the rating curve. Of course, performing frequent control measurements in Greenland has logistic challenges. Nowadays an Acoustic Current Doppler Profiler (ADCP) is the most common instrument to measure discharge in large rivers. Unfortunately, this instrument is sensitive to very high sediment loads occasionally observed in glacial rivers. Prior to using the ADCP-instrument, an observer in a boat used a traditional current propeller to record a number of velocity profiles while stepwise moving the boat across the river. This method is slow and may take several hours. Therefore, it is no surprise that control measurements made from 2008-2010 (Figure 12) scatter much around of the rating curve.

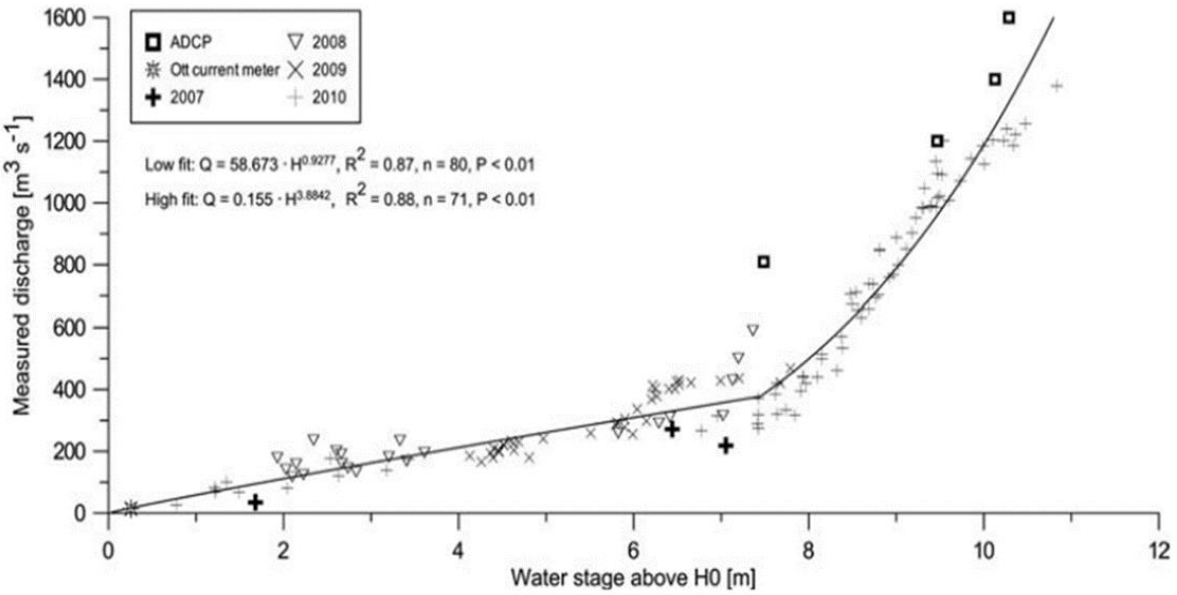

Figure 12. Watson river bridge (Kangerlussuaq) 2010 rating curve. Often the rating curve is presented with stage on the vertical and discharge on the horizontal axis (after Hasholt et al., 2012).

The seasonal variations in solar input result in seasonal variations in discharge as described above. However, the diurnal variations in radiation also results in diurnal variations in discharge as depicted on Figure 13. This influences the variation of all variables that are related to discharge as for instance suspended load.

Finally one can mention that the occurrence of the maximum or minimum in diurnal variation relates to the time in transit between the glacier and the discharge station. Thus on a clear summer day in Sandflugtsdalen maximum discharge at a bridge a few kilometres from the glacier front occurs late afternoon. Contrary to this, the maximum will occur about 6 hours later at the bridge in Kangerlussuaq.

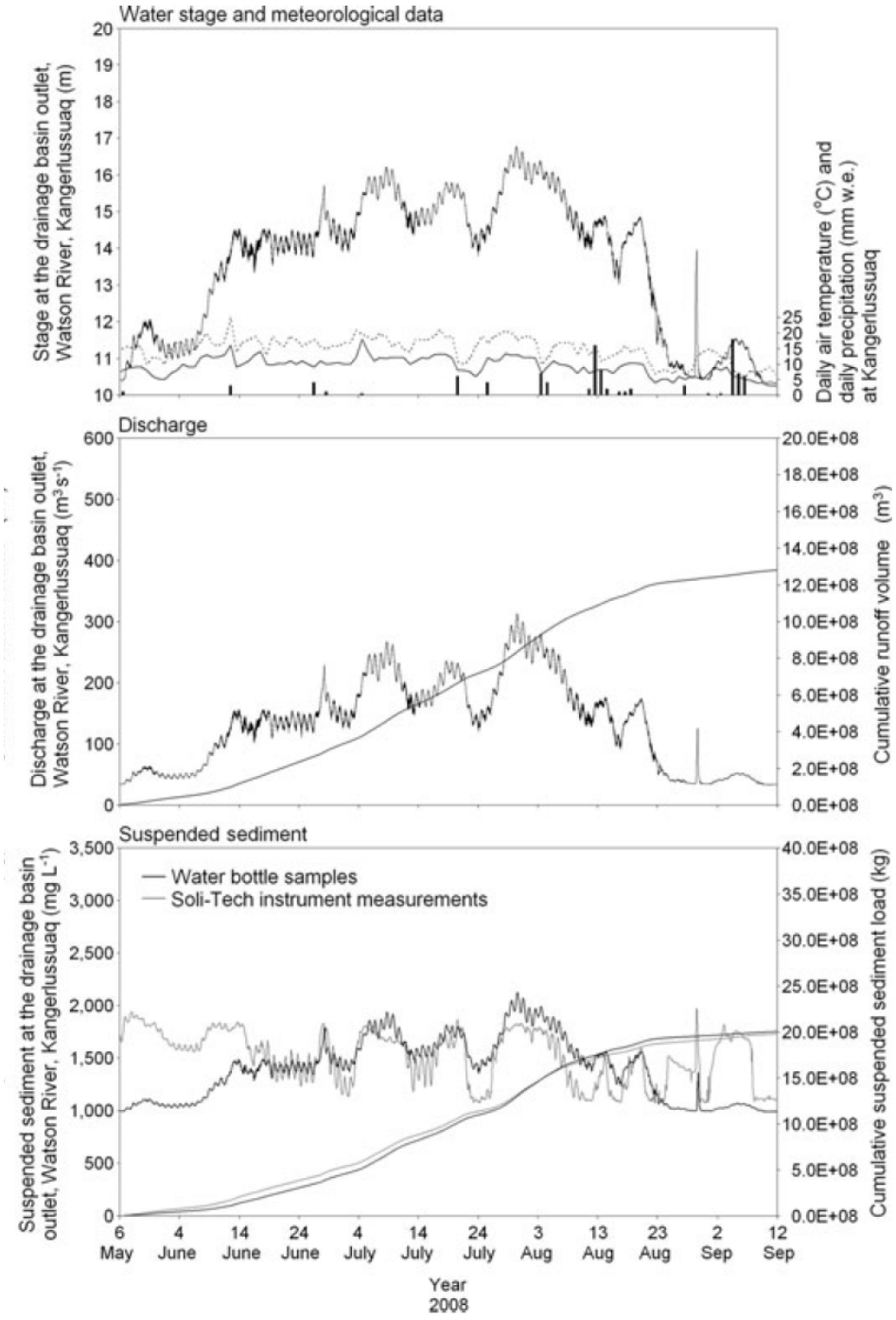

Figure 13. Stage, discharge, meteorological variables and suspended sediment in Watson River, Kangerlussuaq, 2008 (Mernild & Hasholt, 2009)

Dust

The annual variation in discharge results in frequent exposure to wind erosion of silt and sand deposited on the outwash plains formed by the meltwater coming from the GrIS. Generally the occurrence of dust emissions reflects the relative importance and interactions among sediment supply, sediment availability, and transport capacity (Bullard et al. 2011). Sediment supply to the floodplain depends on fluvial sediment supply and exposure of sediment on the floodplain. Therefore, dust emissions may be limited by a lack of suitable sediment. Likewise deflation from glacial outwash plains may also be availability limited; for example, by surface moisture content, vegetation, snow cover, frost, or the development of lag deposits (McKenna Neuman, 1993). Transport capacity is determined by effective wind speed.

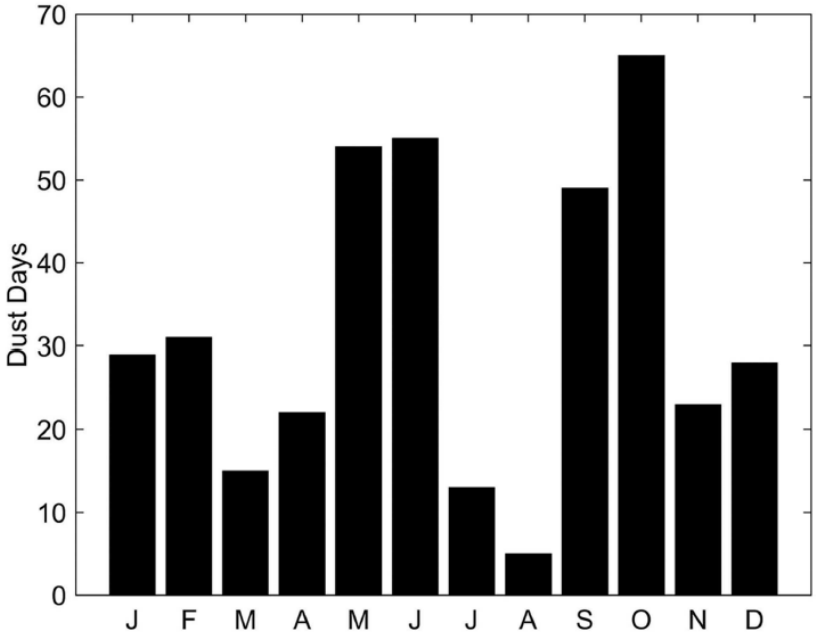

Figure 14. Seasonal variability of dust event days at Kangerlussuaq 1945-2015.

Figure 14 shows that peak dust emissions in Kangerlussuaq occur in spring when snow cover rapidly is decreasing, exposing the sediment that is delivered to the outwash plains to strong winds. As meltwater discharge increases during the summer, a large proportion of the outwash plains may be inundated, reducing deflation potential; at the same time, precipitation increases during the summer, raising surface moisture levels across the landscape and suppressing dust emissions. As discharge and precipitation decrease at the end of the summer (September–October) a large quantity of fine sediment can be left draped across the outwash plains and is susceptible to wind erosion. Snow cover is limited in the Kangerlussuaq region, but freezing of the soil may reduce but not impede dust generation by winter storms.

References

Ambach, A., 1963. Untersuchungen zum Energieumsatz in der Ablationszone des Grönländischen inlandeises. Medd. Grønl., 174 (4) (1963), p. 311.

Bullard, J. E., S. P. Harrison, M. C. Baddock, N. Drake, T. E. Gill, G. H. McTainsh, and Y. Sun. 2011. Preferential dust sources: A geomorphological classification designed for use in global dust models. Journal of Geophysical Research 116. doi:10.1029/2011JF002061.

Bullard, B.E. and Mockford, T., 2018. Seasonal and decadal variability of dust observations in the Kangerlussuaq area, west Greenland, Arctic, Antarctic, and Alpine Research, 50:1, S100011.

Cappelen, J., Jørgensen, B.V., Laursen, E.V., Stannius, L.S. and Thomsen, R.S. 2000. The Observed Climate of Greenland, 1958-99 - with Climatological Standard Normals, 1961-90. Danish Meteorological Institute, Technical Report TR00-18, Copenhagen.

Cappelen, J., 2017: Weather observations from Greenland 1958-2016. Observation data with description. Danish Meteorological Institute, Technical Report TR17-08, Copenhagen.

Hasholt, B., Mikkelsen, A.B.,, Nielsen, M.H. and Larsen,M.A.D., 2012. Observations of Runoff and Sediment and Dissolved Loads from the Greenland Ice Sheet at Kangerlussuaq, West Greenland, 2007 to 2010. Zeitschrift für Geomorphologie, Supplementary Issue. Published online December 2012.

Lindbäck, K., R. Pettersson, A.L. Hubbard, S.H. Doyle, D. van As, A.B. Mikkelsen, and A.A. Fitzpatrick, 2015. Subglacial water drainage, storage, and piracy beneath the Greenland ice sheet, Geophys. Res. Lett., 42, 7606–7614, doi:10.1002/2015GL065393.

McKenna Neuman, C. 1993. A review of aeolian transport processes in cold environments. Progress in Physical Geography 17:137–55. doi:10.1177/030913339301700203. Mernild, S & Hasholt, B., 2009. Observed runoff, Jökulhlaups and suspended sediment load from the Greenland Ice sheet, Kangerlussuaq. Journ. Glaciology, 55, 855-858.

Mernild, S. H., Hanna, E., McConnell, J. R., Sigl, M., Beckerman, A. P., Yde, J. C., Cappelen, J., and Steffen, K. 2015. Greenland precipitation trends in a long-term instrumental climate context (1890–2012): Evaluation of coastal and ice core records. International Journal of Climatology, 35, 303–320, doi:10.1002/joc.3986.

Mernild, S. H., Liston, G. E., van As, D., Hasholt, B., and Yde, J. C. 2018. High-resolution ice sheet surface mass-balance and spatiotemporal runoff simulations: Kangerlussuaq, West Greenland. Arctic, Antarctic, and Alpine Research (Special Issue), doi.org/10.1080/15230430.2017.1415856.

van den Broeke, M. R.; Smeets, C. J. P. P.; and van de Wal, R. S.W. The seasonal cycle and interannual variability of surface energy balance and melt in the ablation zone of the west Greenland ice sheet. The Cryosphere, 5, 377–390, 2011. doi:10.5194/tc-5-377-2011

van De Wal, R.S.W., Greuell, W., van den Broeke, M.R., Reijmer, C. H. and Oerlemans, J., 2005. Surface mass-balance observations and automatic weather station data along a transect near Kangerlussuaq, West Greenland. Annals of Glaciology, 42: 311-316.